

9-1-2020

Application of the Saffir-Simpson Hurricane Wind Scale to Assess Sand Dune Response to Tropical Storms

Jean Taylor Ellis
jtellis@sc.edu

Michelle E. Harris

Mayra A. Román-Rivera

J. Brianna Ferguson

Peter A. Tereszkievicz

See next page for additional authors

Follow this and additional works at: https://scholarcommons.sc.edu/geog_facpub



Part of the [Geography Commons](#)

Publication Info

Published in *Journal of Marine Science and Engineering*, Volume 8, Issue 9, 2020, pages 670-.
© 2020 by the authors. Licensee MDPI, Basel, Switzerland. This article is an open access article distributed under the terms and conditions of the Creative Commons Attribution (CC BY) license (<http://creativecommons.org/licenses/by/4.0/>).

This Article is brought to you by the Geography, Department of at Scholar Commons. It has been accepted for inclusion in Faculty Publications by an authorized administrator of Scholar Commons. For more information, please contact dillarda@mailbox.sc.edu.

Author(s)

Jean Taylor Ellis, Michelle E. Harris, Mayra A. Román-Rivera, J. Brianna Ferguson, Peter A. Tereszkievicz, and Sean P. McGill

Article

Application of the Saffir-Simpson Hurricane Wind Scale to Assess Sand Dune Response to Tropical Storms

Jean T. Ellis *, Michelle E. Harris, Mayra A. Román-Rivera, J. Brianna Ferguson,
Peter A. Tereszkiwicz and Sean P. McGill

Department of Geography, University of South Carolina, Columbia, SC 29208, USA;
mh28@email.sc.edu (M.E.H.); mayrar@email.sc.edu (M.A.R.-R.); jbf2@email.sc.edu (J.B.F.);
petert@email.sc.edu (P.A.T.); spmcgill@email.sc.edu (S.P.M.)

* Correspondence: jtellis@sc.edu; Tel.: +1-803-777-1593

Received: 24 July 2020; Accepted: 18 August 2020; Published: 1 September 2020



Abstract: Over one-third of the Earth's population resides or works within 200 km of the coast. The increasing threat of coastal hazards with predicted climate change will impact many global citizens. Coastal dune systems serve as a natural first line of defense against rising sea levels and coastal storms. This study investigated the volumetric changes of two dune systems on Isle of Palms, South Carolina, USA prior to and following Hurricanes *Irma* (2017) and *Florence* (2018), which impacted the island as tropical storms with different characteristics. *Irma* had relatively high significant wave heights and precipitation, resulting in an average 39% volumetric dune loss. During *Florence*, a storm where precipitation was low and winds were moderate, net volumetric dune loss averaged 3%. The primary driving force causing dune change during *Irma* was water (precipitation and storm surge), and during *Florence*, it was wind (aeolian transport). We suggest that the application of the Saffir-Simpson Hurricane Wind Scale classifications should be reconsidered because different geomorphic responses were measured, despite *Irma* and *Florence* both being designated as tropical storms. Site-specific pre- and post-storm studies of the dune morphology and site-specific meteorological measurements of the storm (wind characteristics, storm surge, precipitation) are critically needed.

Keywords: coastal storms; tropical cyclones; coastal hazards; incipient foredunes; Saffir-Simpson Hurricane Wind Scale; Isle of Palms; South Carolina

1. Introduction

Approximately 3.2 billion people either live or work within 200 km of a coastline [1]. Additionally, it is estimated that more than 200 million people are under threat of extreme sea-level events resulting from coastal storms [2]. During these storms, the beach-dune system serves as a natural defense mechanism for the coastline, which is unfortunately threatened worldwide by storm-induced erosion [3]. Dune response to storms is controlled by storm characteristics and the pre-existing dune morphology [4–7]. Dunes are also weakened from multiple, frequent storm impacts [8–11]. Maintenance of the dunes is imperative not only to the natural environment, but also to the coastal built environment and surrounding communities that provide provisioning, regulatory, cultural, and support functions [12]. Accordingly, understanding the geomorphic response of dune systems to storm events is vital based on the current population distribution, its anticipated growth, and estimations of more frequent and intensifying tropical cyclones [13].

Dunes are a critical sedimentological component of the beach-dune-bar system [14,15]. Storms can have a range of impacts on the dunes, from minor scarping to major overwash or breach events [16,17].

Foredune height and extent, relative to the tidal stage during the storm event, are controlling factors on dune response [16,18,19], and are also directly related to sediment availability [20–23]. Individual characteristics of the storm or dune system can affect the observed geomorphic responses. Generally, they are summarized as the relationships between land elevations, water levels, and the stages of rising storm waters [24].

Many studies have been conducted in barrier island dune systems to describe the observations and mechanisms of storm-based erosion (described in [14]), here we highlight those specific to hurricanes. Pre- and post-*Dennis* (2005) digital elevation models (DEMs) were generated to calculate a 7% volumetric loss along a 2 km long study site along the Florida Panhandle [25]. Following Hurricane *Ivan* (2004, Florida Panhandle), 70% of the incipient foredunes were destroyed and in several of their field study locations, storm overwash was noted [26]. During *Ivan*, it was suggested that wave set-up and swash were the significant contributors to overwash processes and dune erosion [27]. Specific to South Carolina, a 25% volumetric loss and a 9% volumetric gain at 14th and 56th Avenues, respectively, was measured on Isle of Palms following Hurricane *Hugo* (1989) [28]. These surveys were approximately 250 m in shore-perpendicular length (to -1.5 m MSL), and therefore covered the dune, beach, and a portion of the nearshore bar system [28]. Another study investigated *Hugo* along the coast of South Carolina and concluded there was severe beach and dune erosion [29]. They also found that high and continuous dunes served as a solid barrier to coastal inundation [29].

The Saffir-Simpson scale is the industry standard to classify tropical cyclones formed in the Atlantic and northern Pacific (East of the International Date Line). A form of this scale has been used for a half a century since Saffir aimed to provide a similar estimation to the Richter earthquake magnitude scale for hurricane property damage [30]. Simpson enhanced this concept with storm surge estimates, which resulted in the Saffir-Simpson Hurricane Scale (SSHS) [31]. Despite its pervasive use, the SSHS has received substantial criticisms, including saturation at its higher end and issues related to the ‘hard transitions’ between categories, which then have substantial impacts on decision-makers and/or evacuation orders [32]. Following Hurricane *Katrina* (2005), many have proposed alternatives to the SSHS that consider adding maximum storm wind velocity, storm size, storm surge, and/or offshore bathymetry [32–34]. In response, the original SSHS that considered barometric pressure, storm surge, and maximum sustained wind velocity for 1 min was revised in 2010. The new scale, coined the Saffir-Simpson Hurricane Wind Scale (SSHWS), only considers a 1–5 categorical designation of the hurricane, based on the maximum 1 min sustained wind velocity. Unfortunately, the aforementioned ‘hard transition’ issue between the categories was not rectified. However, the SSHWS is used as an indicator to predict coastal geomorphic change [6].

Scant research has acknowledged that variability of coastal morphologic change is related to and/or explained by SSHWS or its predecessor [16], and additional research is needed. However, it has been demonstrated that the interactions between the shoreline, storm, and subsequent coastal response are complex, and that site-specific studies are needed (e.g., [34]). Therefore, this study reports field-based geomorphic assessments of two dune systems on Isle of Palms, SC, USA, before and after Hurricanes *Irma* (2017) and *Florence* (2018). These data are used to determine the storm-based volumetric changes. We also compare these changes to the characteristics of the two tropical storms upon impact with Isle of Palms.

2. Study Area

Isle of Palms (IOP, Figure 1) is a barrier island located 15.5 km northeast of Charleston, SC, USA, and is bordered by Dewees Inlet to the northeast and Breach Inlet to the southwest. It is a drumstick barrier island and a mixed energy coast [35]. The tides are semidiurnal, with an average range of 1.5 m and an average spring tidal range of 2.5 m [36]. Onshore wave heights average 0.6 m, and fine-grained quartz sand transports alongshore from northeast to southwest at average rates of $120,000$ m³/yr [37]. The island’s beaches have been altered by humans since the 1970s [38]. Most notably, there were substantial nourishments to the NE portion of the island towards Dewees Inlet (NE

of 53rd Avenue, Figure 1) in 2010 and 2018 [38]. The 2018 nourishment cost \$13.5 million, spanned ~3.8 km, and comprised 1.282 million m³ of sand [38]. Following hurricanes, it is common on this island to scrape the beach, which is moving sand from the foreshore to the pre-storm foredune line (c.f., [39]).



Figure 1. Study area located on Isle of Palms, SC, USA. The blue and red dots indicate Site A at Pavilion Drive and Site B at 53rd Avenue, respectively. The inset map shows the location of Isle of Palms within SC (red box). Base imagery obtained from Google Earth from September 2018.

Historically, the dunes on the SW end of the island had heights that nearly doubled those found in the NE, at approximately 1.5 and 0.7 m, respectively [35]. The NE end of the island was historically described as unstable and erosional, while the SW end was accretional [40]. Accretion in this area was reinforced by alongshore sediment transport patterns [35] and average low wave energy conditions [41]. However, more recently, the island's SW portion (especially southwest of Site A at Pavilion Drive, Figure 1) is highly erosional (personal observation). There have been high energy events impacting South Carolina annually from 2015–2020. Furthermore, the influence of king tides is increasing (c.f., [39]).

Two dune systems along IOP were investigated. The selected locations are part of a longitudinal study that has been in place since Hurricane *Matthew* (2016) (c.f., [42]). Both sites are located adjacent to public beach access points, one at Pavilion Drive along Front Beach (Site A; Figure 2a) and a second at 53rd Avenue (Site B; Figure 2b). Site A has higher relative pedestrian foot traffic, with 50–150 m of beach in front of the current setback line, depending on the tidal stage [43]. Site B is a wider beach-dune system with 125–190 m of beach-dune complex between the setback line and waterline [43], depending on the tidal stage. This site receives minimal impact from beachgoers because of its proximity to a private, gated community that is located just NE of the study site and extends to the end of the island. Additional details about the dune characteristics are discussed later.

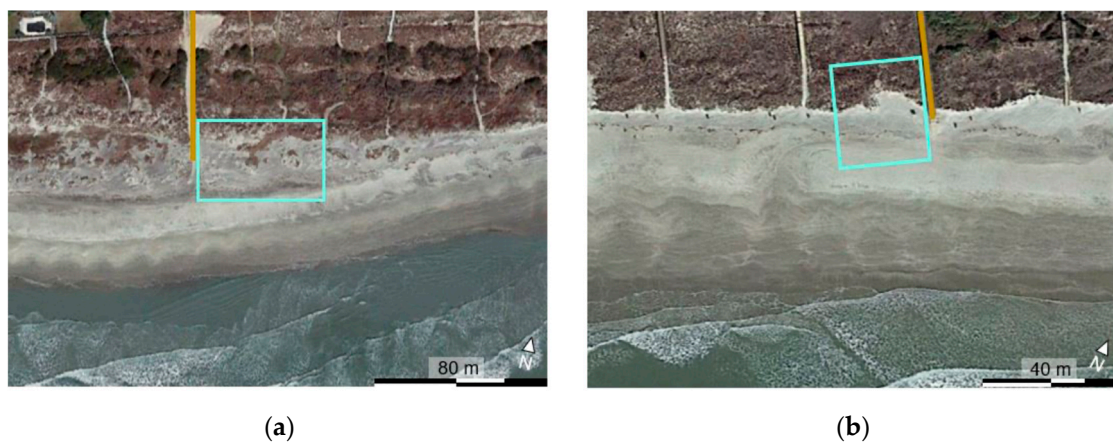


Figure 2. Aerial images of (a) Sites A and (b) B. The yellow colored lines show the location of the pedestrian boardwalk at (a) and the 53rd Avenue beach access (b). Google Earth imagery from March 2018.

3. Hurricanes *Irma* and *Florence*

This study considers Hurricanes *Irma* and *Florence* (Figure 3). At peak intensity, *Irma* was a Category 5 [44] using the SSHWS. *Irma* first made landfall on U.S. soil at Cudjoe Key, Florida as a Category 3 storm. It traveled up the Florida peninsula and dissipated over Missouri. *Florence* was a Category 4 hurricane at its peak intensity according to the SSHWS [45]. *Florence* made landfall at Wrightsville Beach, North Carolina, approximately 240 km from IOP, as a Category 1 hurricane, using the SSHWS. Tropical storm conditions were measured in South Carolina during *Irma* and *Florence*, despite *Irma*'s eye not traveling into the state [44,45].

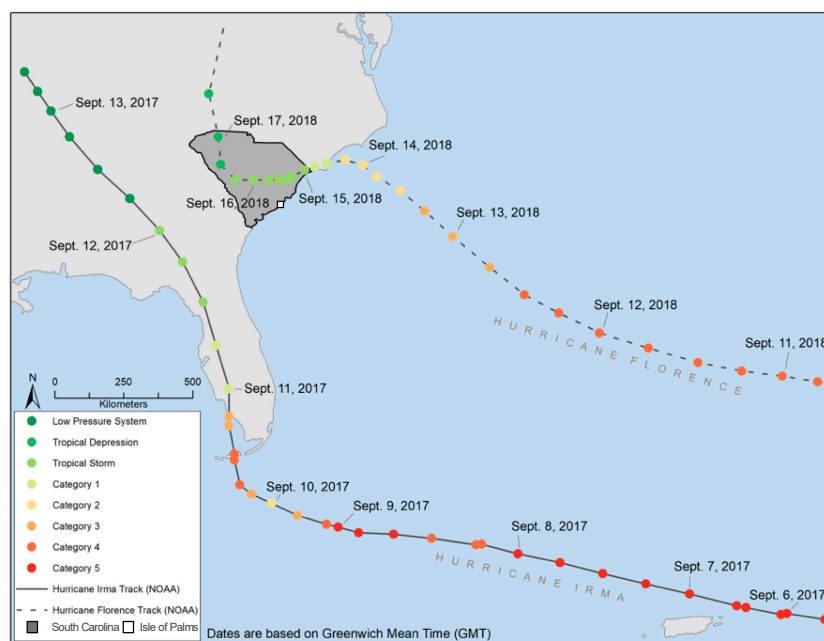


Figure 3. Hurricanes *Irma* and *Florence* path [46,47].

Wind and wave data were obtained from the National Oceanic and Atmospheric Administration’s (NOAA) National Data Buoy Center (NDBC) (Station 41004) to temporally encompass the South Carolina-issued hurricane watches for *Irma* and *Florence* and the field surveys conducted for this study. The hurricane watches were 30 August 2017 to 12 September 2017 for *Irma*, and 30 August 2018 to 18 September 2018 for *Florence*. The field survey protocols are described in Section 3. This NOAA

NDBC station is located 73 km southeast of Breach Inlet (Figure 1) and is the closest instrument suite that simultaneously measures wind and waves. NOAA reports a 20 min average significant wave height every hour. Maximum and average 8 s wind gust speeds, measured during 2 min periods, are reported every 10 min from an anemometer 4.1 m above the surface. The maximum wind gust is from the 10 min time interval. All wind and wave data obtained from the NOAA station are averaged to 3 h time blocks for data presentation purposes. Wind and wave data were used to identify possible forcing events, herein defined as $>2\sigma$ of the hurricane watch temporal duration. The $>2\sigma$ threshold has been used by other researchers, including those studying dunes at IOP [39,48,49]. Figure 4 shows the NOAA Station 41004 data where the 2σ threshold significant wave heights, wind speeds, and wind gusts during the hurricane watch are denoted by arrows. The temporal duration of the hurricane watch and the date of storm impact on IOP are also noted.

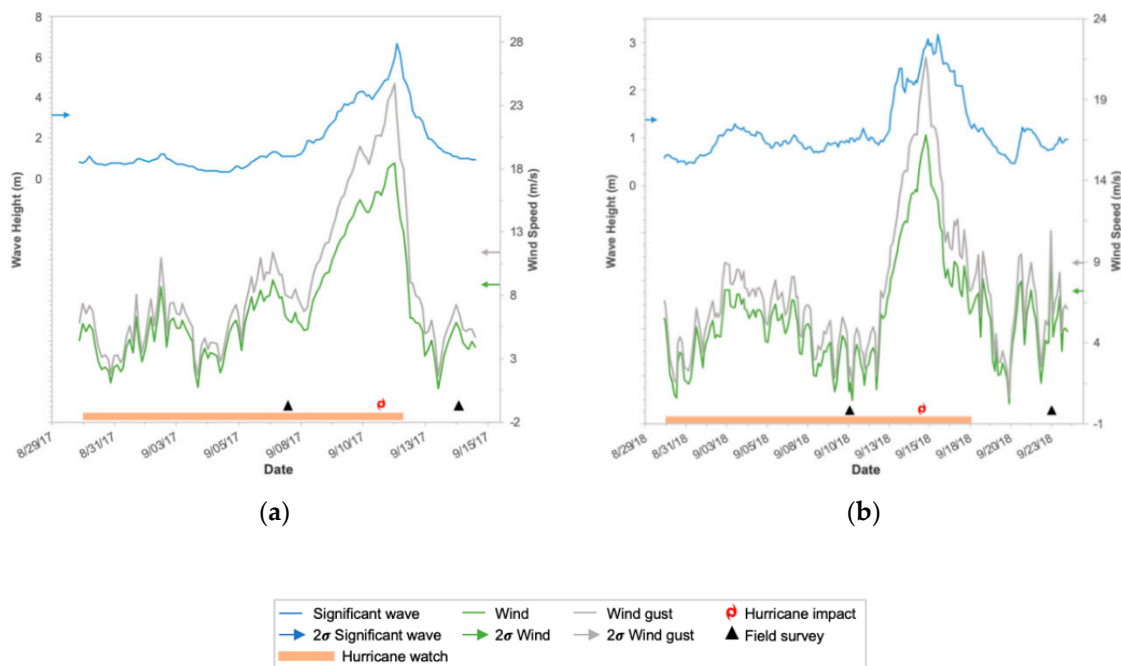


Figure 4. Significant wave heights, wave speeds, and wind gusts during the (a) *Irma* and (b) *Florence* study periods.

Irma weakened to a tropical storm as it approached the U.S. Southeast. It did not make landfall on the coast of South Carolina, but impacted IOP on 11 September 2017. Mean wind speeds were 7.3 m/s and bidirectional, with peak wind gusts of 30.1 m/s from the NE (Table 1). The Charleston Community Collaborative Rain, Hail & Snow Network (CoCoRaHS) sites recorded an average of 184.25 mm rainfall during the storm [44]. The peak storm surge (storm tide minus the astronomical tide) at the Charleston NOAA National Ocean Service gauge was 1.28 m MHHW [44]. The peak storm tide observed at Charleston Harbor was the third-highest on record at that time, as the storm impacted IOP approximately at high tide [50]. Table 1 provides a summary of storm conditions for Hurricanes *Irma* and *Florence*, as they pertain to conditions on, or nearest available to, IOP.

Table 1. Summary storm conditions during *Irma* and *Florence* obtained from the closest instrument(s) to Isle of Palms.

		<i>Irma</i>	<i>Florence</i>
SSHWS		Tropical storm	Tropical Storm
Wind Speed (m/s)	Average	7.3 *	6.0 *
	2 σ	8.9 *	7.2 *
Wind Gust (m/s)	Average	9.4 *	7.6 *
	2 σ	11.5 *	9.0 *
	Maximum	30.1 *	23.6 *
Dominant Storm Wind Direction		NE *	SSW *
Significant Wave Height (m)	Average	1.8 *	3.1 *
	2 σ	1.3 *	1.4 *
Storm Surge (m) MHHW		1.28 °	0.45 #
Storm Precipitation Total (mm)		184.25 °	31.75 #

* NOAA Station 41004; ° [44]; # [45].

Similarly to *Irma*, *Florence* weakened from a hurricane to a tropical storm before impacting IOP on 15 September 2018 when the tides were low. Mean wind speeds were 6.0 m/s (predominantly from the SSW), with peak wind gusts measured at 23.6 m/s that were predominantly from the SSW (NOAA Station 41004; Table 1). *Florence* was a slow, forward-moving storm along its path. This resulted in large precipitation totals and devastating floods, which were evident in north South Carolina and North Carolina [45]. However, closer to the IOP study site (at the Charleston airport), less rain was measured (31.75 mm) during the storm [45]. The peak storm surge at the NOAA’s National Ocean Service Charleston gauge was 0.45 m MHHW [45].

4. Assessing Dune Change

Field data collection was executed prior to and after each storm at Sites A and B. Pre- and post-*Irma* data collection was conducted on 7 and 14 September 2017. The pre-hurricane *Florence* survey took place on 10 September 2018, and the post-*Florence* survey was conducted on 23 September 2018.

Topographic data were obtained using a Sokkia Series 30R Total Station, which has an instrument accuracy of +/-2 mm. Points were recorded approximately every meter and at geomorphic breaks along shore-perpendicular transects. At Site A, eight transects were spaced 6.5 m apart over a shore parallel length of 44.5 m (Figure 2a). At Site B, ten transects were spaced 5.5 m apart over a shore parallel length of 55 m (Figure 2b). There was an average of 165 points at Site A and an average of 265 points at Site B recorded during each survey. Site B is a wider beach-dune system in the cross-shore and alongshore directions. Benchmarks and the total station locations were established using an X90-OPUS Static GPS receiver that has a +/-5 mm instrument accuracy.

This study focuses on the dunes, however, measurements were also obtained (and presented) for the beach to understand the erosion and accretion of both systems. The onshore extents of Sites A and B are landward of the pre-Hurricane *Matthew* primary foredune, and are the same baselines that were used by others at the same field sites [42]. The offshore extents of the dunes are defined according to the dune toes, which are dynamic and defined as where there is a distinct change in slope between the dune and backshore. The offshore extents of the beaches are static. The intervening space between the dune toes and the offshore beach lines comprise a narrow zone of the upper backshore that is not inundated by tides. It is recognized that the beach definition used in this paper is not traditional, and it is not the same that is used by others [14,51]. However, there is precedent when studying the same IOP system for using these same beach and dune definitions [42].

The survey points were used to create digital elevation models (DEMs) and DEM-based change maps to estimate beach and dune volumetric change using the above-mentioned beach and dune definitions. DEMs were generated using the ordinary kriging method, with cell and lag sizes of 0.2 m. The semivariogram model was spherical. The average RMSEs for Sites A and B were 0.03 m and 0.02 m,

respectively. These averages do not include the Site A post-*Irma* survey because changing the backsite resulted in an RMSE of 0.15 m. The DEM plane height was -1.0 m for both sites. Normalized DEM volumes were calculated by dividing the post-storm by pre-storm volumes. DEM change maps are valuable to identify regions of erosion and accretion over time, which in this case is pre- to post-storm conditions. However, exact survey points and field notes were used to identify the dune toe line.

5. Results

5.1. Site A Beach-Dune System

Before Hurricane *Irma* at Site A, the dune system was generally characterized as a foredune that was recovering following Hurricane *Matthew* (2016) (c.f., [42]). It was a rounded dune ridge with no defined scarp. Vegetation was abundant onshore of the dune crest and portions of the offshore dune slope (Figure 5a–c). Hurricane *Irma* scarped the dune resulting in a near-vertical slope with exposed roots (Figure 5d–f). The storm deposited beach wrack offshore of the post-storm dune toe (Figure 5d–f). The DEM change map (Figure 6a) shows almost consistent spatial volumetric gain onshore of the post-storm dune toe line. Substantial volumetric loss was observed directly onshore of the pre-storm dune toe line. The lateral onshore dune toe erosion from *Irma* ranged from 2.0 to 8.5 m. The total range of change from *Irma*, using a DEM change map was 2.51 m (-1.19 to 1.32 m).

The pre-*Florence* photographs show that the *Irma* storm scarp is still present and that slumping occurred during the last year (Figure 5g–i). The details of the intervening time between *Irma* and *Florence* are beyond the scope of this paper, but addressed elsewhere (c.f., [42]). Pioneering stabilizing species, such as *Hydrocotyle bonariensis*, were present along the pre-storm dune toe. The most noticeable geomorphic change post-Hurricane *Florence* was the depositional lobe at the scarp base (Figure 5j–l). This depositional lobe is best illustrated in Figure 5i,l that compare the pre- and post-storm conditions and show the post-storm vegetation burial. The *Florence* DEM change map reveals a complex pattern of erosion and deposition ranging from 0.44 to -0.59 m. The post-storm depositional lobe on the NE side of the site (noted above) is captured by the DEM change map (Figure 6b, green box). The DEM change map also reveals erosion along the SW portion of the site. From a quantitative perspective, Site A had a greater loss in dune volume following *Irma* (28%), compared to the volume loss following *Florence* that was statistically negligible (Table 2). There was minimal lateral dune toe change when comparing pre- and post-storm conditions, the maximum retreat approximated 0.5 m.

Table 2. Dune volumes (m^3 and normalized volumes (*nv*)) for pre- and post-*Irma* and *Florence* for Sites A and B.

	<i>Irma</i>		<i>Florence</i>	
	Pre-	Post-	Pre-	Post-
SITE A				
Volume (m^3)	1762.2	1437.1	1488.9	1482.1
<i>nv</i>	1.00	0.82	1.00	1.00
SITE B				
Volume (m^3)	4934.6	2017.3	2953.5	2772.7
<i>nv</i>	1.00	0.41	1.00	0.94



Figure 5. Site A field photographs showing conditions (a–c) pre-*Irma*, (d–f) post-*Irma*, (g–i) pre-*Florence*, and (j–l) post-*Florence*. Symbology denotes anthropogenic or natural locations that are consistent to more than one photograph.

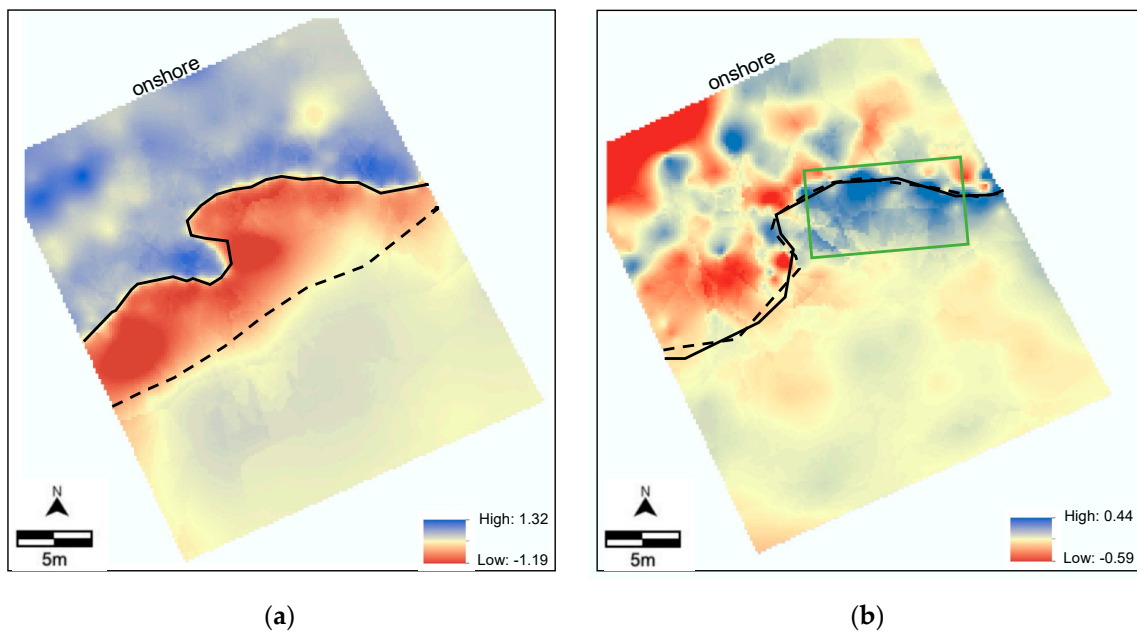


Figure 6. Site A digital elevation models (DEM) change maps for Hurricanes (a) *Irma* and (b) *Florence*. The dashed and solid lines show the pre- and post-storm dune toe lines, respectively.

5.2. Site B Beach-Dune System

Before Hurricane *Irma* at Site B, there was an incipient dune field with new-growth vegetation (Figure 7a,b). Hurricane *Irma* eroded the offshore portion of the incipient dune field, leaving behind storm wrack (Figure 7c,d). The DEM change map (Figure 8a) confirms the substantial dune erosion. Four shore-parallel incipient foredunes were eliminated, resulting in a maximum of 1.41 m of erosion (Figure 8a, green box). The onshore portion of the study site experienced accretion (up to 0.40 m), with that sand concentrated around a few mounds toward the NE and SE extremes (Figure 8a). Table 2 shows that the normalized volume decreased substantially from 1.00 to 0.41 from the pre- to post-*Irma* surveys. The onshore, lateral dune retreat from *Irma* ranged from 12.0 to 20.0 m.

Prior to *Florence*, the incipient foredune system was visually similar to the pre-*Irma* condition, with new-growth vegetation present (Figure 7e,f). Field observations and the corresponding photographs (Figure 7g,h) suggested that the site was minimally impacted by *Florence*. The solitary vegetation patch visible before and after the storm (Figure 7e,g) remained intact. However, the DEM change map (Figure 8b) reveals a complex spatial pattern of volumetric gains and losses. The magnitude of change ranges from 0.10 to -0.54 m, which is substantially smaller compared to the other location and scenarios considered. Table 2 codifies this low magnitude change; the normalized volume was 0.94. The onshore dune toe retreat from *Florence* was minimal, with an average onshore regression of approximately 1.0 m. The normalized post-storm volume changes at this site were 0.41 for *Irma* and 0.94 for *Florence*.

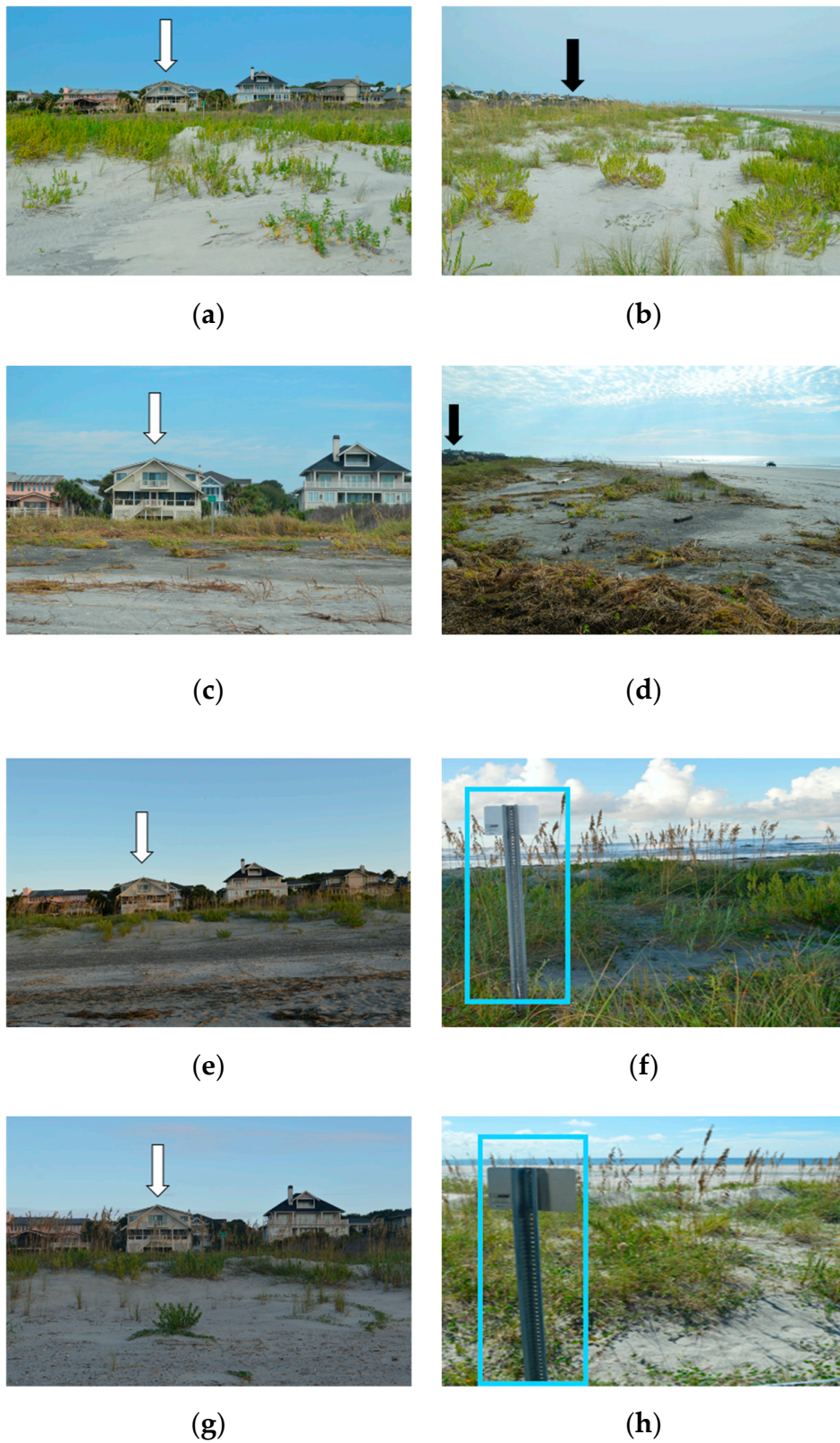


Figure 7. Site B field photographs showing conditions (a,b) pre-Irma, (c,d) post-Irma, (e,f) pre-Florence, and (g,h) post-Florence. Symbology denotes anthropogenic or natural locations that are consistent to more than one photograph.

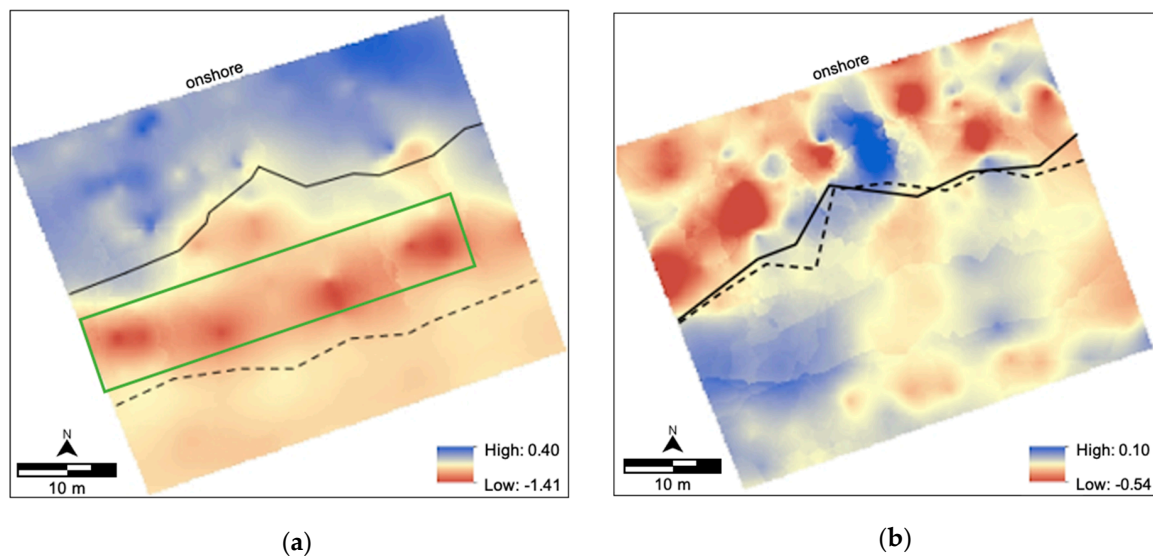


Figure 8. Site B DEM change maps for Hurricanes (a) *Irma* and (b) *Florence*. The dashed and solid lines show the pre- and post-storm dune toe lines, respectively.

6. Discussion

Hurricanes *Irma* and *Florence* impacted the IOP dunes as tropical storms with similar intensities based on SSHWS. However, analysis of the storm characteristics (Table 1 and Figure 4) suggests that the overall system energetics were substantially less for *Florence* compared to *Irma*, except for significant wave height (despite the closer geographic proximity of *Florence* to the field site). For example, during *Irma*, the maximum and average wind gust was 28% and 24% higher, respectively (Table 1). In addition, the precipitation and storm surge was 574% and 284% higher during *Irma* (Table 1). Figure 4 strongly suggests that the storm energetics were limited to the duration of *Irma* and *Florence* and that no substantial geomorphic changes were likely outside the temporal duration of either storm. These data also exemplify the variability of conditions observed in situ, even within the ‘tropical storm’ classification. Accordingly, even though both systems impacted the IOP dunes as tropical storms (i.e., the same SSHWS designation), *Irma* and *Florence* resulted in different geomorphic responses. This suggests that the geomorphic changes resulting from *Irma* are most indicative of water-based processes and geomorphic changes from *Florence* are largely related to wind-driven, or aeolian processes. The following paragraphs justify this statement and discuss each storm to highlight the different responses with an emphasis on the relationships between the geomorphic change and the dominant forcing factor(s).

Hurricane *Irma* impacted IOP at approximately high tide. A substantial amount of rain fell (184 mm, Table 1), which prohibited aeolian transport, despite the high wind speeds (c.f., [52] for review on the negative impact of moisture on aeolian transport potential). Both sites experienced dune erosion and volumetric loss (averaging 39%), with patterns suggestive of rising water levels and associated storm surge. However, the geomorphic response was different at Site A compared to Site B. The scarping at Site A was likely caused by rising water levels, as evidenced by the high angled slopes (Figure 5d–f). At this site, there was extensive dune scarping (up to 8.5 m); this erosion is the main contributor to the minimum DEM value of -1.2 m and a volumetric loss of 18%. At Site B, *Irma* substantially decreased the total volume of sediment (pre- and post-storm normalized values of 1.00 and 0.41, respectively). The storm-induced erosion was concentrated on four incipient foredunes that decreased in elevation by approximately 1.4 m, from what we believe was the storm surge. The dune toe regressed by up to 20 m. The deposition on the onshore portion of the site was distributed (with a maximum of 0.40 m elevation change) and concentrated to previously low-lying areas. Based on our observations and the associated data analyses, we surmise that during *Irma*, the IOP dunes

were most strongly influenced by storm-associated water damage, which was a combination of high tides, storm surge, and precipitation.

When Hurricane *Florence* impacted IOP, the tide was low with obliquely onshore winds (SSW dominant and gusts peaking at 23.6 m/s), and precipitation was limited to ~32 mm (Table 1). The post-storm geomorphic response showed that the dune toe line minimally changed at both sites. At Site A, an accumulation of dry sand was observed offshore of the post-storm dune toe (Figure 6b (grey box)), suggesting that aeolian processes were paramount. A visible gap between the scarp and this accumulation of sand (visible on Figure 5l) strongly suggests that the sand source was offshore of the scarp. However, the NE side of the dune scarp (the right side of the DEM) showed evidence of post-storm deposition, which is consistent with onshore winds. Holistic analysis of this site reveals no net volumetric change when comparing pre- and post-storm conditions (normalized volume change of 1.00). Hurricane *Florence* had minimal impact on Site B. A majority of the post-storm deposition was observed onshore of the dune toe line (within the incipient foredunes), which suggests aeolian transport. We therefore surmise that resulting from *Florence*, the IOP dunes were most strongly influenced by aeolian transport, which also explains the minimal net geomorphic change.

The immediate morphologic response dunes of IOP, following *Irma* and *Florence*, can be compared to other dune systems following hurricanes. At Site B (*Irma*) the incipient foredunes were devastated, which is similar to the response of the incipient foredunes along the Florida coast after *Ivan* [26]. Similar to *Ivan*, we surmise that the *Irma* damage is largely from water [27]. *Hugo* is considered the 'benchmark' storm of the South Carolina coast because of its devastation to IOP and the entire South Carolina coast [28,29]. A previous study [28] reported beach-dune volumetric changes for ~250 m transects (~10x longer than those in this study). Net erosion and accretion were found along the transects closest to our study sites [28]. The dune volumetric loss reported here was 39% for *Irma* and 3% for *Florence*.

7. Conclusions

General assumptions are made about tropical storm intensities and the associated, potential dune damage. For example, the United States Geologic Survey (USGS) Coastal Change Hazards Portal [53] predicts dune damage according to SSHWS. The pre- and post-storm morphologic data (Table 2, Figures 5–8) from two dune sites on Isle of Palms, SC related to two tropical storms (*Irma* and *Florence*) suggest that the general assumptions are misguided because dramatically different geomorphic responses were measured, and these were the same storm category. Our findings are similar to previous research that concluded that stronger tropical cyclones do not equate with greater morphologic coastal change [16].

The findings from this study reveal that the precipitation-dominant *Irma* (as observed on IOP), which also had relatively high significant wave heights, and impacted the Island during high tide, resulted in an average 39% volumetric loss of the IOP dunes. During *Florence*, a storm where precipitation and the tides were low, winds were moderate, and aeolian transport geomorphically impacted the dunes, the net volumetric change was inconsequential (average of 3% volumetric loss). We therefore attest that not only is the magnitude of the tropical storm important, which is summarized by SSHWS, but also the characteristics of the storm, such as wave height, storm surge, wind speed, and precipitation. The latter are not components of SSHWS, but should be in future iterations. In the meantime, the SSHWS should be applied with caution when predicting or characterizing morphologic change of beach-dune systems.

This research emphasizes the importance of not overlooking site-specific geomorphic and meteorological measurements. *Florence*, because of its slow-forward moving speed, resulted in catastrophic flooding over parts of North and South Carolina (c.f., [54]). However, IOP was spared from this devastation. Interestingly, *Irma* produced more precipitation on the island in comparison, affirming the need for the site-specific meteorological measurements. We attest that site-specific measurements of coastal topography, wind characteristics, waves, storm surge, and precipitation should be ascertained.

The research presented herein exhibits that when investigating dune morphology immediately prior to, and following storms, generalizations based on the application of the SSHWS classification are over-simplified. Specifically, during *Irma*, the IOP dunes were most strongly influenced by high tides, storm surge, and precipitation. During *Florence*, the IOP dunes were most strongly influenced by aeolian transport, which was possible due to adequate wind speeds and minimal precipitation. This research demonstrated that two tropical storms impacting Isle of Palms, SC resulted in systematically different geomorphic impacts to the coastal dune system (*Irma* = −39%; *Florence* = −3%). We aspire that future studies will reconsider the application of SSHWS and will include site-specific geomorphic and meteorological measurements, all of which will not only benefit academic research, but also will support and improve coastal management decisions.

Author Contributions: Conceptualization, J.T.E.; methodology, J.T.E., M.A.R.-R.; formal analysis, J.T.E., M.E.H.; field-based data collection, J.T.E., M.A.R.-R., S.P.M., M.E.H., P.A.T., J.B.F; data curation, M.E.H., M.A.R.-R.; writing—original draft preparation, J.T.E.; writing—review and editing, J.T.E.; M.E.H.; M.A.R.-R.; P.A.T.; J.B.F.; S.P.M.; visualization, M.E.H.; J.T.E.; J.B.F.; supervision and project administration, J.T.E. All authors have read and agreed to the published version of the manuscript.

Funding: This research was partially supported by the Department of Geography at the University of South Carolina and HVRI.

Acknowledgments: J.T.E would like to thank IOP Fire Chief Ann Graham, IOP Mayor Jimmy Carroll, and Linda Tucker for their cooperation and support of this research. The research team appreciates the many that helped us in the field: Erika Chin, Holly Gould, April Hiscox, and Alexandria McCombs. J.T.E. and M.E.H. thank ALE and PPC for their unconditional support during this study.

Conflicts of Interest: The authors declare no conflict of interest. The funders had no role in the design of the study; in the collection, analyses, or interpretation of data; in the writing of the manuscript, or in the decision to publish the results.

References

1. The Coastal Population Explosion. Available online: http://oceanservice.noaa.gov/websites/retiredsites/natdia_pdf/3hinrichsen.pdf (accessed on 8 September 2018).
2. Nicholls, R.J. Planning for the impacts of sea level rise. *Oceanography* **2011**, *24*, 144–157. [CrossRef]
3. Harley, M.D.; Ciavola, P. Managing local coastal inundation risk using real-time forecasts and artificial dune placements. *Coast. Eng.* **2013**, *77*, 77–90. [CrossRef]
4. Hall, M.J.; Halsey, S.D. Comparison of overwash penetration from Hurricane Hugo and pre-storm erosion rates for Myrtle Beach and North Myrtle Beach, South Carolina, USA. *J. Coast. Res.* **1991**, *SI8*, 229–235.
5. Claudino-Sales, V.; Wang, P.; Horwitz, M.H. Factors controlling the survival of coastal dunes during multiple hurricane impacts in 2004 and 2005: Santa Rosa Barrier Island, Florida. *Geomorphology* **2008**, *95*, 295–315. [CrossRef]
6. Plant, N.G.; Stockdon, H.F. Probabilistic prediction of barrier-island response to hurricanes. *J. Geophys. Res. Earth Surf.* **2012**, *117*. [CrossRef]
7. Houser, C.; Wernette, P.; Rentschlar, E.; Jones, H.; Hammond, B.; Trimble, S. Post-storm beach and dune recovery: Implications for barrier island resilience. *Geomorphology* **2015**, *234*, 54–63. [CrossRef]
8. Coco, G.; Senechal, N.; Rejas, A.; Bryan, K.R.; Capo, S.; Parisot, J.P.; Brown, J.A.; MacMahan, J.H.M. Beach response to a sequence of extreme storms. *Geomorphology* **2014**, *204*, 493–501. [CrossRef]
9. Karunarathna, H.; Pender, D.; Ranasinghe, R.; Short, A.D.; Reeve, D.E. The effects of storm clustering on beach profile variability. *Mar. Geol.* **2014**, *348*, 103–112. [CrossRef]
10. Dissanayake, P.; Brown, J.; Wisse, P.; Karunarathna, H. Effect of storm clustering on beach / dune erosion. *J. Geol.* **2015**, *370*, 63–75.
11. Angnuureng, D.B.; Almar, R.; Senechal, N.; Castelle, B.; Addo, K.A.; Marieu, V.; Ranasinghe, R. Shoreline resilience to individual storms and storm clusters on a meso-macrotidal barred beach. *Geomorphology* **2017**, *290*, 265–276. [CrossRef]
12. Everard, M.; Jones, J.; Watts, B. Have we neglected the societal importance of sand dunes? An ecosystem services perspective. *Aquat. Conserv.* **2010**, *20*, 476–487. [CrossRef]

13. Webster, P.J.; Holland, G.J.; Curry, J.A.; Chang, H.R. Changes in tropical cyclone number, duration, and intensity in a warming environment. *Science* **2005**, *5742*, 1844–1846. [[CrossRef](#)]
14. Houser, C.; Ellis, J. Morphodynamic systems: Beach and dune interaction. In *Treatise on Geomorphology*; Schroder, J., Sherman, D.J., Eds.; Academic Press: San Diego, CA, USA, 2013; pp. 267–288.
15. Román-Rivera, M.A. Innovative Approaches Using Multispectral Imagery to Detect Nearshore Bars and Elucidate Beach System Dynamics. Ph.D. Thesis, University of South Carolina, Columbia, SC, USA, 2019.
16. Sallenger, A.H. Storm impact scale for barrier islands. *J. Coast. Res.* **2000**, *16*, 890–895. [[CrossRef](#)]
17. Hesp, P. Foredunes and blowouts: Initiation, geomorphology and dynamics. *Geomorphology* **2002**, *48*, 245–268. [[CrossRef](#)]
18. Thieler, E.R.; Young, R.S. Quantitative evaluation of coastal geomorphological changes in South Carolina after Hurricane Hugo. *J. Coast. Res. Spec. Issue* **1991**, *8*, 187–200. [[CrossRef](#)]
19. Houser, C.; Hapke, C.; Hamilton, S. Controls on coastal dune morphology, shoreline erosion and barrier island response to extreme storms. *Geomorphology* **2008**, *100*, 223–240. [[CrossRef](#)]
20. Leatherman, S.P. Barrier island dynamics: Overwash processes and eolian transport. In *Coastal Engineering 1976, Proceedings of the 15th International Conference*; American Society of Civil Engineers: Reston, VA, USA, 1976; pp. 1958–1974.
21. Leatherman, S.P. Barrier dune systems: A reassessment. *Sediment. Geol.* **1979**, *24*, 1–16. [[CrossRef](#)]
22. Armon, J.W. Dune erosion and recovery on a northern barrier. In *Coastal Zone '80, Proceedings of the 2nd Symposium on Coastal and Ocean Management*; American Society of Civil Engineers: Reston, VA, USA, 1980; pp. 1233–1250.
23. Psuty, N.P. Spatial variation in coastal foredune development. In *Coastal Dunes: Geomorphology, Ecology and Management for Conservation*; Carter, R.W.G., Curtis, T.G.F., Sheehy-Skeffington, M.J., Eds.; Balkema: Rotterdam, The Netherlands, 1992; pp. 3–13.
24. Morton, R.A. Factors controlling storm impacts on coastal barriers and beaches—A preliminary basis for near real-time forecasting. *J. Coast. Res.* **2002**, *18*, 486–501.
25. Priestas, A.M.; Fagherazzi, S. Morphological barrier island changes and recovery of dunes after Hurricane Dennis, St. George Island, Florida. *Geomorphology* **2010**, *114*, 614–626. [[CrossRef](#)]
26. Claudino-Sales, V.; Wang, P.; Horwitz, M.H. Effect of Hurricane Ivan on coastal dunes of Santa Rosa Barrier Island, Florida: Characterized on the basis of pre- and poststorm LIDAR surveys. *J. Coast. Res.* **2010**, *26*, 470–484. [[CrossRef](#)]
27. Wang, P.; Kirby, J.H.; Haber, J.D.; Horwitz, M.H.; Knorr, P.O.; Krock, J.R. Morphological and sedimentological impacts of Hurricane Ivan and immediate poststorm beach Recovery along the Northwestern Florida barrier-island coasts. *J. Coast. Res.* **2006**, *226*, 1382–1402. [[CrossRef](#)]
28. Katuna, M.P. The effect of Hurricane Hugo on the Isle of Palms, South Carolina: From destruction to recovery. *J. Coast. Res. Spec. Issue* **1991**, *8*, 263–273.
29. Coch, N.K.; Wolff, M.P. Effects of Hurricane Hugo storm surge in coastal South Carolina. *J. Coast. Res.* **1991**, *SI*, 201–226.
30. Saffir, H.S. Hurricane wind and storm surge. *Military Eng.* **1973**, *423*, 4–5.
31. Simpson, R.H. The hurricane disaster-potential scale. *Weatherwise* **1974**, *27*, 169–186.
32. Kantha, L. Time to replace the Saffir-Simpson Hurricane Scale? *Eos Trans. Am. Geophys. Union* **2006**, *87*, 3–6. [[CrossRef](#)]
33. Powell, M.D.; Reinhold, T.A. Tropical cyclone destructive potential by integrated kinetic energy. *Bull. Am. Meteorol. Soc.* **2007**, *88*, 513–526. [[CrossRef](#)]
34. Anthony, E.J. Geomorphology storms, shoreface morphodynamics, sand supply, and the accretion and erosion of coastal dune barriers in the southern North Sea. *Geomorphology* **2013**, *199*. [[CrossRef](#)]
35. Hayes, M.O.; Moslow, T.F.; Hubbard, D.K. *Beach Erosion in South Carolina*; Coastal Research Division, Department of Geology, University of South Carolina: Columbia, SC, USA, 1978; p. 99.
36. Tides & Currents: Isle of Palms Pier, SC—Station ID 8665494. Available online: <https://tidesandcurrents.noaa.gov/stationhome.html?id=8665494> (accessed on 24 July 2020).
37. Kana, T.W. Beach erosion during minor storms. *J. Waterway Port Coast. Ocean Division* **1977**, *103*, 505–518.
38. CSC (Coastal Science & Engineering). *Final Report 2018 Beach Restoration Project City of Isle of Palms*; Technical Report #CSE-2453FR; CSE: Columbia, SC, USA, 2018; p. 57.

39. Ellis, J.T.; Román-Rivera, M.A. Assessing natural and mechanical dune performance in a post-hurricane environment. *J. Mar. Sci. Eng.* **2019**, *7*, 126. [[CrossRef](#)]
40. Stephen, M.F.; Brown, P.J.; Fitzgerald, D.M.; Hubbard, M.K.; Hayes, M.O. *Beach Erosion Inventory of Charleston County, South Carolina: A Preliminary Report*; Technical Report No. 4; S.C.; Sea Grant: Charleston, SC, USA, 1975; p. 79.
41. Fico, C. Influence of Wave Refraction on Coastal Geomorphology - Bull Island to Isle of Palms, South Carolina. Master's Thesis, Coastal Research Division, Department of Geology, University of South Carolina, Columbia, SC, USA, 1978; p. 190.
42. Ellis, J.T.; Román-Rivera, M.A.; Harris, M.E.; Tereszkiwicz, P.A. Two years and two hurricanes later: Did the dunes recover? *Shore & Beach* **2020**. (in print).
43. South Carolina Department of Health and Environmental Control-Ocean & Coastal Management (SCDHEC-OCRM). SC Beachfront Jurisdictional Lines. Available online: <https://gis.dhec.sc.gov/shoreline/> (accessed on 5 May 2020).
44. Cangialosi, J.P.; Latta, A.S.; Berg, R. National Hurricane Center Tropical Cyclone Report: Hurricane Florence (AL112017). National Hurricane Center. 30 June 2018. p. 111. Available online: https://www.nhc.noaa.gov/data/tcr/AL112017_Irma.pdf (accessed on 21 December 2019).
45. Stewart, S.R.; Berg, R. National Hurricane Center Tropical Cyclone Report: Hurricane Florence (AL062018). National Hurricane Center. 30 May 2019. 2019; p. 98. Available online: https://www.nhc.noaa.gov/data/tcr/AL062018_Florence.pdf (accessed on 21 December 2019).
46. National Hurricane Center and Central Pacific Hurricane Center. NHC GIS Archive – Tropical Cyclone Best Track for AL 11207. Available online: https://www.nhc.noaa.gov/gis/archive_besttrack_results.php?id=al11&year=2017&name=Hurricane%20IRMA (accessed on 1 July 2020).
47. National Hurricane Center and Central Pacific Hurricane Center. NHC GIS Archive – Tropical Cyclone Best Track for AL 062018. Available online: https://www.nhc.noaa.gov/gis/archive_besttrack_results.php?id=al06&year=2018&name=Hurricane%20FLORENCE (accessed on 1 July 2020).
48. Harris, M.E.; Ellis, J.T.; Barrineau, C.P. Evaluating the geomorphic response from sand fences on dunes impacted by hurricanes. *Ocean Coast. Manage* **2020**. (in print). [[CrossRef](#)]
49. Zhang, K.; Douglas, B.; Leatherman, S.; The, S.; July, N.; Zhang, K.; Douglas, B.; Leatherman, S. Do storms cause long-term beach erosion along the U.S. east barrier coast? *J. Geol.* **2002**, *110*, 493–502. [[CrossRef](#)]
50. National Weather Service (NWS). Tropical Storm Irma–September 10–11, 2017. Available online: <https://www.weather.gov/chs/TropicalStormIrma-Sep2017f> (accessed on 9 March 2020).
51. Masselink, G.; Hughes, M.G. *Introduction to Coastal Geomorphology and Processes*; Arnold: London, UK, 2003; p. 354.
52. Ellis, J.T.; Sherman, D.J. Fundamentals of aeolian sediment transport: Wind blown sand. In *Treatise on Geomorphology*; Schroder, J., Lancaster, N., Sherman, D.J., Baas, A.C.W., Eds.; Academic Press: San Diego, CA, USA, 2013; Volume 11, pp. 85–108.
53. USGS Coastal Change Hazards. Available online: <https://marine.usgs.gov/coastalchangehazardsportal/> (accessed on 9 March 2020).
54. Griffen, M.; Malsick, M.; Mizzell, H.; Moore, L. Historic rainfall and record-breaking flooding from Hurricane Florence in the Pee Dee Watershed. *J. South Carolina Water Res.* **2019**, *6*, 28–35. [[CrossRef](#)]

